

Nonlinear and Snap-Through Responses of Curved Panels to Intense Acoustic Excitation

C. F. Ng*

NASA Langley Research Center, Hampton, Virginia

Assuming a single-mode transverse displacement, a simple formula is derived for the transverse load-displacement relationship of a plate under in-plane compression. The formula is used to derive a simple analytical expression for the nonlinear dynamic response of postbuckled plates under sinusoidal or random excitation. The highly nonlinear motion of snap-through can be easily interpreted using the single-mode formula. Experimental results are obtained with buckled and cylindrical aluminum panels using discrete frequency and broadband excitation of mechanical and acoustic forces. Some important effects of the snap-through motion on the dynamic response of the postbuckled plates are described. Static tests were used to identify the deformation shape during snap-through.

Nomenclature

K	= linear modal stiffness of the flat plate
P	= externally applied modal force
p	= nondimensional force parameter, $= P/KQ_p$
Q	= modal displacement
Q_p	= value of Q at $R = 1$
q	= nondimensional displacement parameter, $= Q/Q_p$
R	$= \lambda - 1$ (the buckling parameter)
u	= in-plane edge shortening displacement
u_c	= value of u at which buckling starts
λ	$= u/u_c$ (the compression parameter)
Ω	= linear circular frequency of the flat plate
ζ	= modal damping coefficient

Introduction

A TYPICAL aircraft panel can be initially curved or subsequently curved due to mechanical or thermal stresses. If a plate is curved, the static and dynamic behavior in the transverse direction can be highly nonlinear. The nonlinearity can take the form of a hardening spring, a softening spring, or an instability condition with snap-through motion. Previous work on nonlinear response due to intense broadband acoustic excitation was mainly confined to the hardening-spring behavior of flat panels.¹⁻⁵ The only extensive experimental work on nonlinear response of curved panels subject to acoustic excitation was done by Jacobson and Maurer,⁶ Holthouse,⁷ and Ng and White.⁸

The acoustic responses of cylindrical panels were found to be greatly affected by dynamic snap-through motion,⁹ therefore better understanding of snap-through motion is needed to predict the dynamic response of curved panels. Theoretical and experimental results of large-amplitude vibration of postbuckled plates under sinusoidal excitation were obtained by Yamaki and Chiba¹⁰; however, snap-through motion was not studied.

The characteristics of snap-through motion in a postbuckled beam under sinusoidal excitation were studied by Tseng

and Dugundji.¹¹ A theoretical study of the random response of an initially curved beam including snap-through motion was done by Seide.¹² However, a thorough and straightforward understanding of the nonlinear behavior (particularly snap-through motion) of general curved plates is difficult to gather from the previous research results. The present study was conducted to fill this gap using a single-mode analysis method and experimental investigation with sinusoidal and random excitation forces on a buckled plate.

General Formulas for Nonlinear Behavior of Plates

Assuming an appropriate shape function for the transverse displacement of a plate and using the Rayleigh-Ritz procedure of formulation, the nonlinear equation for equilibrium in the transverse direction is obtained. The detailed steps in deriving the following formulas are found in Ref. 13. A brief summary is described in the Appendix.

Equation for Equilibrium in the Transverse Direction

For a plate under uniaxial compression with uniform edge displacement, the nondimensional relationship between modal displacement and modal force for the buckling mode is given as

$$q^3 - Rq = p \quad (1a)$$

for static equilibrium and

$$\ddot{q}/\Omega^2 + 2\zeta\dot{q}/\Omega + q^3 - Rq = p \quad (1b)$$

for dynamic motion.

The preceding formula is applicable to any plate of any boundary condition and aspect ratio if there is no coupling between the various modes. A plot of p vs q for various values of R from Eq. (1a) is shown in Fig. 1. From Fig. 1, regions of hardening- and softening-spring behavior are found, and there are also regions of negative stiffness (e.g., between A and B). Notice that for $R = 1$, dynamic motion starting from C will pass through A and B and end up at C' . This motion through the instability region is called snap-through. A and B are found to be at $(0.577, -0.385)$, $(-0.577, 0.385)$, respectively, by locating the points where $dp/dq = 0$.

Static equilibrium positions q_0 under R are found by putting $p = 0$ in Eq. (1) and correspond to the points where the curve crosses the q axis in Fig. 1. Note that for postbuckling region $R > 0$ there are three equilibrium values of

Received June 13, 1988; revision received Sept. 21, 1988. Copyright © 1988 American Institute of Aeronautics and Astronautics, Inc. No copyright is asserted in the United States under Title 17, U.S. Code. The U.S. Government has a royalty-free license to exercise all rights under the copyright claimed herein for Governmental purposes. All other rights are reserved by the copyright owner.

*Resident Research Associate, Structural Acoustics Branch. Member AIAA.

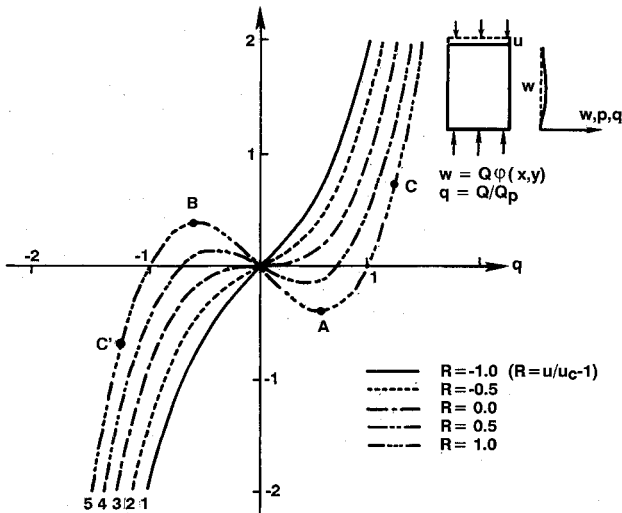


Fig. 1 Plots for transverse force equilibrium equation of a plate under in-plane compression.

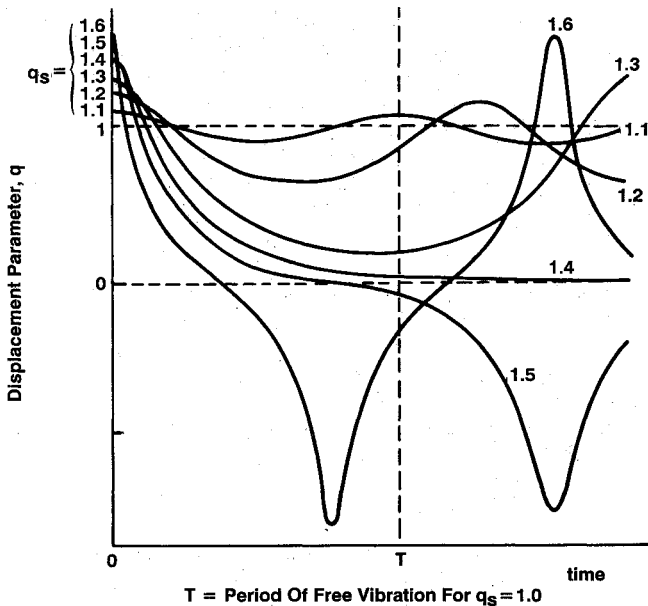


Fig. 2 The free vibration of a postbuckled plate for different magnitudes of initial displacements q_s , $R = 1$ ($u/u_c = 2$), $q_o = 1$.

$q:q_o = \sqrt{R}$, $-\sqrt{R}$, and zero. The last value (zero) is an unstable position as the stiffness is negative. We can rewrite Eq. (1) in terms of the postbuckling displacement q_o as

$$q^3 - q_o^2 q = p \quad (2a)$$

$$\ddot{q}/\Omega^2 + 2\zeta\dot{q}/\Omega + q^3 - q_o^2 q = p \quad (2b)$$

Undamped Free Vibration of Postbuckled Plate

From Eq. (2b), by neglecting damping terms and applied force, the free vibration equation is

$$\frac{1}{\Omega^2} \ddot{q} + (q^3 - q_o^2 q) = 0 \quad (3)$$

With the substitution $\dot{q} = \dot{q} dq/dq$, Eq. (3) can be integrated to obtain \dot{q} . For the initial conditions $\dot{q}(0) = 0$ and

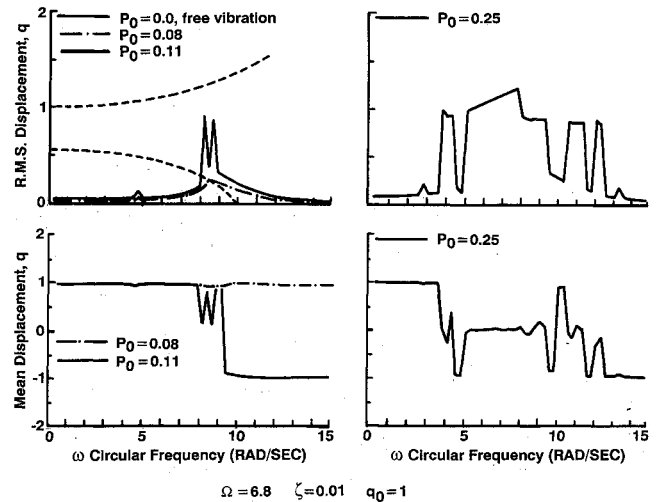


Fig. 3 The forced vibration response of a buckled plate.

$q(0) = q_s (q_s > q_o)$ at $t = 0$, the equation can be written

$$Q^2 = \frac{\Omega^2}{2} (q_s^2 - q^2)(q_s^2 + q^2 - 2q_o^2) \quad (4)$$

Solving Eq. (4) for \dot{q} by numerical integration (see Ref. 13), time histories for the free vibration of various initial values of $q(q_o = 1)$ were determined and are shown in Fig. 2. When $q_s < \sqrt{2}$, it can be seen that the period of vibration increases with initial amplitude and the motion is not symmetrical about the static position. Also note that for $q_s = 1.3$, stable oscillation is possible, although the motion goes into the region of negative stiffness, where q is between -0.577 and 0.577 (as given in Fig. 1). When $q_s = \sqrt{2} = 1.414$, the period is theoretically infinite, as it takes infinite time to approach zero. However, when $q_s > \sqrt{2}$, the period decreases with increase of amplitude. The displacement also passes through both equilibrium positions, $q = 1$ and $q = -1$, indicating snap-through motion. The change of mean position is q_o (from 1 to 0). Also, the rms value is approximately 1 (the static value) when $q_s = 1.5$. Essentially, the postbuckled plate shows softening-spring behavior initially and hardening-spring behavior after snap-through motion.

Forced Sinusoidal Vibration of the Postbuckled Plates

The numerical time integration method is used to find the nonlinear response of the postbuckled plates under sinusoidal force. The Runge-Kutta technique is used to analyze the equation of motion of a buckled plate [Eq. (2b)] with $\zeta = 0.01$, $\Omega = 6.8$, $q_o = 1$, $p = p_o \sin \omega t$, where p_o and ω are the amplitude and circular frequency of the excitation force, respectively. Note that the linear natural circular frequency of the buckled plate $= \sqrt{2}\Omega = 10.0$.

First, p_o is equal to zero, and the free vibration responses are found for various initial values of q (just like in the previous section on undamped free vibration). The natural frequencies are plotted against the corresponding rms values as the dashed line in Fig. 3a. The lower branch of the curve is for vibration about the static position $q = 1.0$. The upper branch is for snap-through motion about the flat position $q = 0.0$. Increasing the amplitude of vibration from zero, the curve starts from $\omega = 10.0$ and ends in $\omega = 0.0$ in the lower branch. Snap-through motion occurs when q (rms) exceeds 0.6 at $\omega = 0$, and then q (rms) reaches 1.0 and ω increases with the amplitude.

When $p_o = 0.08$ and ω decreases from 15.0 to 0.0, the forced response (the broken line in Fig. 3a) is typical of a softening spring and the peak response is near the free

vibration curve. The mean values of q do not change considerably (see the broken line in Fig. 3b).

When $p_o = 0.11$, snap-through occurs at $\omega = 8.25$ and 8.75 (the solid line in Figs. 3a and 3b), as indicated by q (rms) = 0.9 (close to 1.0) and q (mean) = 0.07 (close to zero). Note that the snap-through motion does not start at $\omega = 0$, the frequency of free vibration when snap-through starts. Under the forced vibration condition, instability occurs when q (rms) reaches 0.35 before q (rms) gets to 0.6, for which $\omega = 0$ in free vibration. The resonance peak tends to jump to the upper branch of the free vibration curve (dashed line), bypassing the free vibration curves in the region $\omega < 8.0$.

When p_o is increased to 0.25, steady and continuous snap-through motion occurs for $5.0 \leq \omega \leq 7.75$ (Figs. 3c and 3d) as indicated by q (mean) = 0. Unsteady snap-through motion (a chaotic motion) occurs at $4.0 \leq \omega \leq 4.5$ and $\omega = 8.0$, as indicated by fluctuating q (mean) values, which are close to but not equal to zero. The q (mean) is not equal to zero because the snap-through motions are intermittent.

Random Vibration

The method of equivalent linearization can be used to solve the nonlinear forced vibration equation from Eq. (2b):

$$\frac{1}{\Omega^2} \ddot{q} + 2 \frac{\zeta}{\Omega} \dot{q} + (q^3 - q_0^2 q) = p \quad (5)$$

The mean square displacement of a buckled plate $\langle q^2 \rangle$ due to white noise excitation with spectral density S_{pp} can be obtained for small and large magnitudes (derived in Ref. 13).

For small excitations $\alpha \leq 0.45q_0^4$ ($\alpha = \pi\Omega S_{pp}/4\zeta$, where α is a nondimensional force parameter, there is no snap-through in the motion,

$$\langle q^2 \rangle = (-q_0^2 + \sqrt{q_0^4 + 3})/3 \quad (6)$$

and q (mean) $\approx q_o$. For $\alpha \geq 2q_0^4$, there is persistent snap-through motion in almost every cycle of oscillation,

$$\langle q^2 \rangle = (q_0^2 + \sqrt{q_0^4 + 12\alpha})/6 \quad (7)$$

and q (mean) = 0. For $0.45q_0^4 < \alpha < 2q_0^4$, snap-through motion is intermittent, and the mean position and mean square values are very unsteady. However, the mean square value can be taken approximately from interpolation between the two endpoints—the point of no snap-through and persistent snap-through motion.

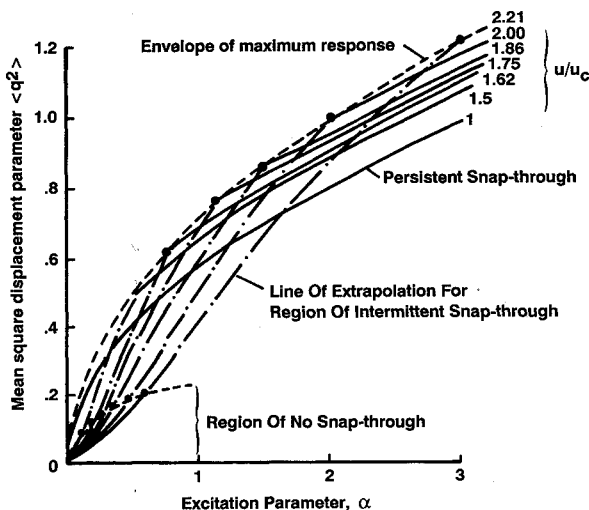


Fig. 4 The variation of displacement response with excitation level in a postbuckled plate.

From Eqs. (6) and (7), for $q_o = 1$, the variation of $\langle q^2 \rangle$ with the excitation parameter α for different values of compression parameter $\lambda(u/u_c)$ is shown in Fig. 4. The rate of increase of response with excitation is highest when intermittent snap-through motion starts. When persistent snap-through motion is attained, the response increases much more slowly with increases in excitation, showing hardening-spring behavior.

From Fig. 4 and Eqs. (6) and (7), the variation of response with compression parameter for various levels of excitation are plotted, as shown in Fig. 5. For a given excitation level, the response increases with compression as it approaches the buckling point. After initial postbuckling, persistent snap-through occurs, and the response continues to increase until a certain point for which only intermittent snap-through motion can be induced. After that point, the response decreases with further increases in compression. The point of maximum displacement corresponds to the point for which the excitation is just sufficient for persistent snap-through motion. Also, the point of maximum response occurs at increasingly greater

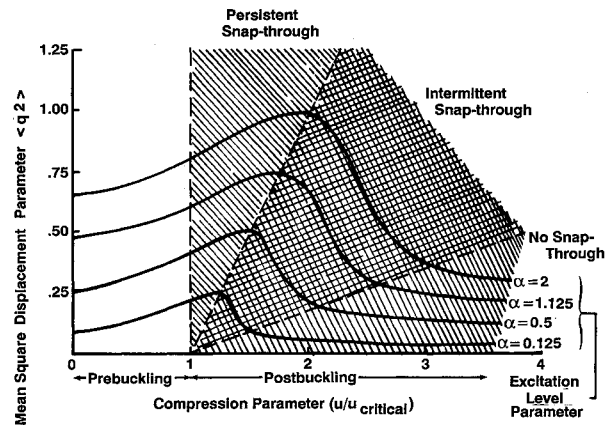


Fig. 5 The variation of displacement response of postbuckled plates under white noise excitation.

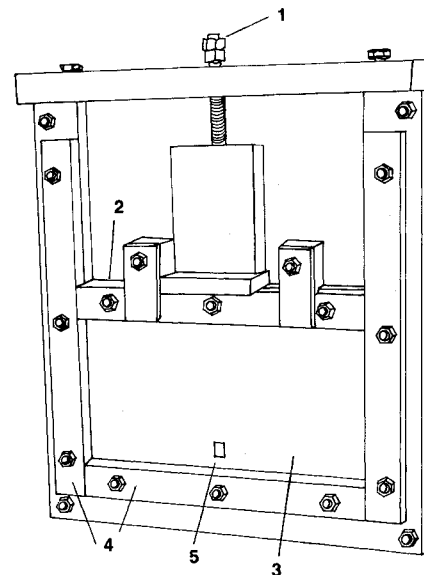


Fig. 6 The loading rig: 1) screw for controlling compression; 2) sliding clamping bar; 3) specimen; 4) clamping bars for sides and bottom edge; 5) strain gage.

plate curvatures, or larger values of u/u_c , as the excitation level increases. These trends have also been predicted in a qualitative description by Jacobson.¹⁴ It should be noted that it is difficult to avoid snap-through motion when the curvature is small, because it requires only low excitation level to excite. However, the magnitude of snap-through motion is also small. Thus, it is also important to find the magnitude of response after snap-through as well as to find the exact limiting point of no snap-through.

Experimental Results with Electromagnetic Shaker

Test Setup

A loading frame with a screw mechanism was used to apply uniform end shortening u to a specimen (Fig. 6). Dynamic tests on several $4 \times 8 \times 0.032$ -in.-thick aluminum plates were carried out using point excitation at the center of the plate by an electromagnetic shaker. Displacement response was measured by the bending strain at the midpoint of the bottom edge. The strain gages were mounted to measure strain in the direction normal to the edge (Fig. 6). By arranging the pair of back-to-back strain gages (on two sides of the plate) in the bridge circuit so that the output is equal to the difference of the surface strain between the upper and lower surfaces, only the bending strain was measured, and the membrane strain was canceled. Since bending strain = thickness $\times \partial^2 w / \partial x^2$, and assuming single-mode displacement, the strain measured is proportional to Q . Thus, nondimensional strain parameter

$$S = \frac{\text{strain measured}}{\text{strain at } R = 1} = \frac{\text{displacement measured}}{\text{displacement at } R = 1} = q$$

Random Response

The variation of mean square strain parameter ($= \langle S^2 \rangle = \langle q^2 \rangle$) with compression parameter is shown in Fig. 7. The general trend agrees well with predicted results from the single-mode formula (Fig. 5), and the points of maximum responses are near the curve for static values. However, there is a large discrepancy between the experimental results and theoretical prediction for an excitation level of $\alpha = 6$, which indicates that the single-mode representation used in the analysis overpredicts the stiffness of the buckled plate. More modes may be required to represent the deformation pattern and give a lower overall stiffness value. Thus, the single-mode formulas are shown to be inaccurate for large deflection, but they do predict the general trend of the nonlinear characteristics.

Experimental Results with Acoustic Excitation of Buckled Plates

Test Setup

The panel used previously in mechanical excitation was installed in the NASA Langley Thermal Acoustic Fatigue Apparatus (Fig. 8) and subjected to a grazing incident progressive wave acoustic field at levels up to 165 dB. Both static and dynamic components of the bending strain, ϵ microstrain, were measured at the midpoint of the bottom edge of the panel. Note that the surface strain due to bending is $\epsilon/2$.

Broadband Excitation

Comparison of Strain Response of Flat and Buckled Plates

Time histories of the total strain were measured for sound levels from 140–165 dB for two panel configurations, one with the panel flat and unbuckled ($u = 0$) and one with the panel in a curved, buckled configuration ($u = 7u_c$). The static strain measured in the buckled configuration was 5000 microstrain.

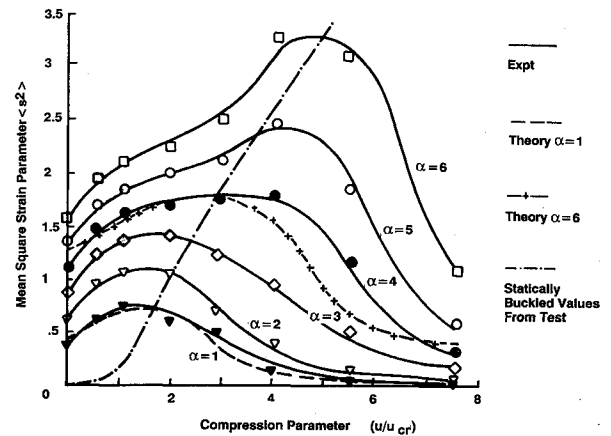


Fig. 7 Variation of random strain response with increasing compression in an isotropic plate ($4 \times 8 \times 0.032$ in., aluminum alloy, edges clamped).

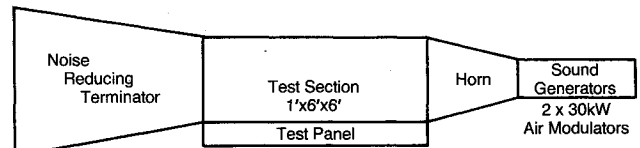


Fig. 8 The thermoacoustic fatigue apparatus.

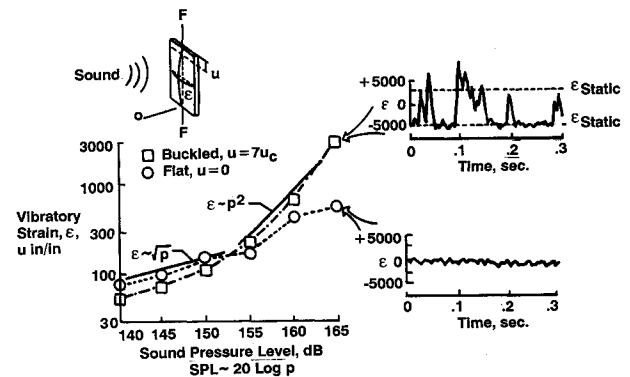


Fig. 9 The acoustic responses of flat and buckled plates ($4 \times 8 \times 0.04$ in.³, aluminum alloy, edges clamped).

The vibratory component of the strain is shown at the lower left of Fig. 9. For the lower sound levels (SPL < 155 dB), the vibratory strain in the buckled panel is less than that in the flat panel. This results from the greater stiffness due to curvature in the buckled panel. At these levels both curves follow a square-root trend, indicating hardening-spring nonlinear response. At levels above 155 dB, the strain increases rapidly with sound level for the buckled panel, following a trend to the square of the sound pressure, indicating softening-spring response. The time history at the upper right shows that the panel frequently snaps through from the static equilibrium position with $\epsilon = -5000$ to the other static equilibrium position with $\epsilon = +3000$ and back again, causing large vibratory strain values. In contrast, the flat panel (lower right) vibrates only in the neighborhood of the flat position with $\epsilon = 0$.

Comparison of Strain Response for Different Compression

Figure 10 shows the variation of strain parameter with different compression parameters. For a given level of excitation, the maximum response is found at a certain buckled

configuration for which continuous snap-through motion cannot be maintained. This general trend agrees well with predicted results from the single-mode formula (Fig. 5). Note that for SPL of 145 dB, the increase of response due to snap-through is less than that for 166 dB SPL, although the snap-through motions are excited at smaller curvature.

Comparison of Strain Spectrum at Increasing SPL

Figure 11 shows the variation of strain response spectrum with SPL for $u/u_c = 0.0$, i.e., the flat configuration. The response at 60 Hz dominates the response for all SPL. Some of the peak in the spectrum may not be resonance peak but may be due to standing wave in the sound excitation.

For $u/u_c = 2.5$, the response spectrum at low frequency (5–20 Hz) increases faster than response at 80 Hz, and at 154 dB SPL, the peak response at 5 Hz is much higher than that at 80 Hz. This seems to suggest snap-through motion at 0 Hz, as indicated in the free vibration response in Fig. 2. However, forced vibration responses (Fig. 3) from theory suggest that snap-through motion starts at a much higher frequency. Examination of the time histories of the response does not indicate any snap-through for frequency less than 10 Hz (in Fig. 12 in the next section). Thus, the sudden increase of response at 5 Hz is not correlated to excitation at 5 Hz and is probably due to intermittent snap-through motion. When the snap-through motion is continuous, the oscillation consists mainly of snap-through motion of 50 Hz, as shown in the responses at 160 and 166 dB SPL, which show peaks at 50 Hz. For $u/u_c = 7$, an SPL of 166 dB is only sufficient to initiate intermittent snap-through motion, and there is a very sharp peak of the strain response around 5 Hz (Fig. 11a).

Time Histories of the Random Response

The time history of the strain response of the buckled plate of $u/u_c = 2.5$ is found to exhibit stable oscillation around the static value of -3000 microstrain (Fig. 12a) when the SPL is 146 dB. Occasional jumps in the magnitude of vibration occur under an SPL of 154 dB, but the overall mean value is still -3000 microstrain (Fig. 12b). Under an SPL of 160 dB, there is frequent snap-through motion from the initial static value to the alternative static value of $+1400$ microstrain (Fig. 12c), but there is still a lot of oscillation around the initial static value. The overall mean and rms values are very unsteady and are -1992 ± 200 , 1512 ± 150 , respectively. With the excitation increased to 166 dB SPL, the snap-through motion occurs in almost every cycle of oscillation (Fig. 12d), and the period is approximately 0.020 s, which means 50 Hz. This is in agreement with Fig. 11b, which shows a peak at 50 Hz for 166 dB SPL. The rms value of the strain response is 1992 microstrain, which is 66% of the initial static value, 3000 microstrain, but is close to half of the difference between the initial static value and the alternative static value -1600 . The difference between the magnitude of the static values is due to the presence of imperfection in the plate. The mean value of the strain response is -768 microstrain, which is about 25% of the initial static value but is close to the halfway point between the two static values.

Discrete Frequency Excitation

Sinusoidal sound of discrete frequency is used to excite a postbuckled plate of $R = 2.5$ with static bending strain of 3000 microstrain. Snap-through motion is most readily excited by sound excitation of 42 Hz. At 164 dB SPL, the oscillation is essentially a sinusoidal motion of rms value 666 microstrain around the static value (Fig. 13). At 164.5 dB SPL, the oscillation becomes unsteady, showing chaotic motion. At 165 dB SPL, the mean value of the oscillation is shifted to about -2074 microstrain, and the motion is not symmetric about the mean value and is not a pure sinusoidal motion. At 166 dB SPL, the snap-through motion is com-

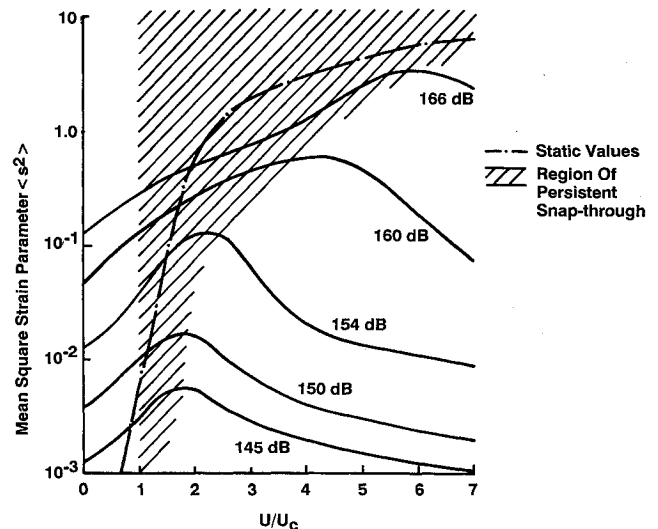


Fig. 10 The comparison of acoustic responses of a plate under different compressions.

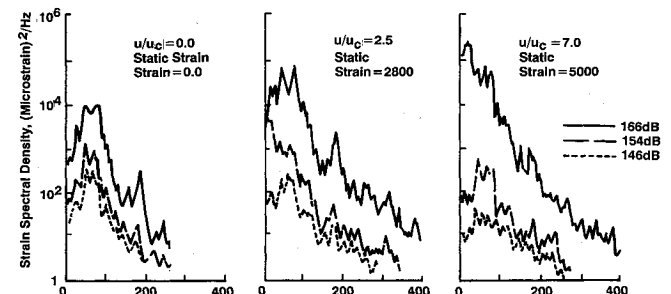


Fig. 11 The comparison of acoustic responses of a plate under different SPL's.

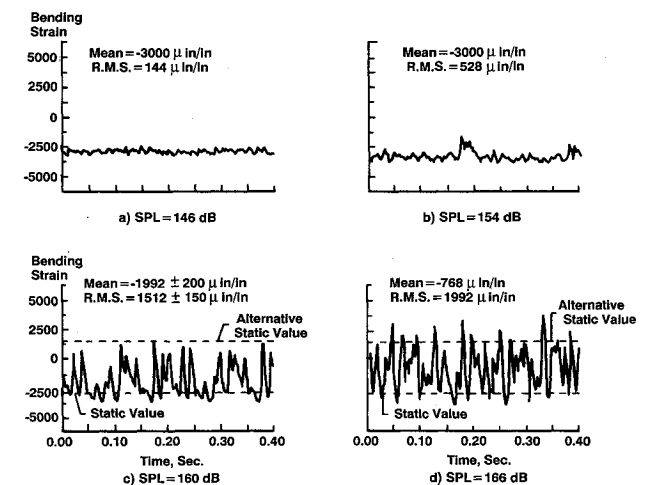


Fig. 12 The time history of the response of a postbuckled plate to random acoustic excitation.

pleted and has a mean of -554 microstrain (only 18% of the static value), and it looks almost like a sinusoidal motion. The rms value of the dynamic strain is 2398 microstrain, 80% of the static value. The snap-through motion at 166 dB is 3.6 times that of the response at 164 dB.

Prediction of Magnitude of Random Response

From the given results, it can be concluded that the magnitude of response with snap-through is related to the initial

Table 1 Effects of snap-through motion on acoustic response

	None	Intermittent	Persistent
Mean	Static value	Unsteady	Zero
rms	<20% static value	Jumps with SPL	>70% of static value
Spectrum	Modal	Peak at 0 Hz	Minor peak
Nonlinearity	Softening	Unstable	Hardening

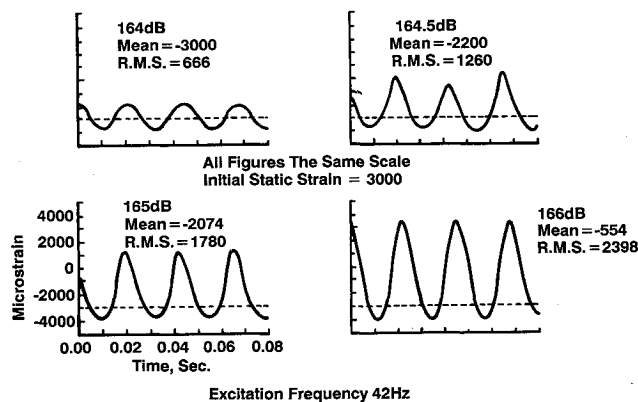


Fig. 13 Snap-through motion of a buckled plate under sinusoidal excitation.

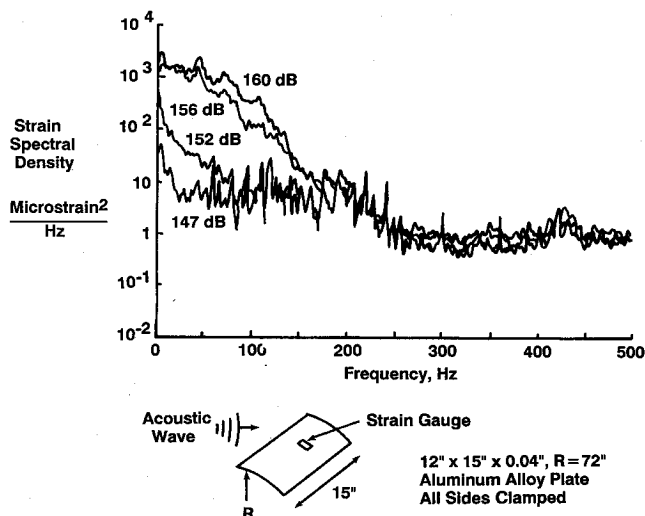


Fig. 15 The acoustic response of a cylindrical panel.

static curvature (Figs. 12 and 13). For large curvature ($u/u_c = 7$, Fig. 9), the effect of snap-through is significant. For small curvature ($u/u_c < 2$, Fig. 10), the snap-through motion can be excited at a low excitation level, but its effect on the response is small. To avoid snap-through motion in slightly curved plates is thus difficult and unnecessary. Previous work^{11,12,14} that studied only cases without snap-through could not provide sufficient design data. By including snap-through in the theoretical prediction, design against fatigue can be based on limiting the response magnitude rather than simply avoiding snap-through motion. The influence of snap-through on the random response is summarized in Table 1.

Static Test

To obtain the mode shapes of the plate during snap-through motion, static tests of snap-through using a transverse point-loading mechanism were conducted. The point loading was applied at the center of the plate to simulate the overall effect of acoustic forces. The deformation shape of the buckled plate during the process of snap-through was recorded by means of the Moire shadow technique. It was found that the snap-through of the (1, 1) symmetric mode is via the intermediate antisymmetric (2, 1) modes, as shown in Fig. 14. This implies that the presence of asymmetry in the acoustic force or the initial static configuration will help initiate the snap-through motion. Also, prediction of the (2, 1) mode during snap-through motion requires the inclusion of both (1, 1), (2, 1) modes in the theoretical analysis.

Experimental Results with Acoustic Excitation of Cylindrical Panel

Acoustic tests were made on a cylindrical panel 15 in. long, 0.04 in. thick, and with curved edges 12 in. wide. The radius of curvature is 72 in. All the edges are clamped. Snap-through behavior as indicated by change of mean value of strain is found at an SPL of 152 dB. The strain response spectrum

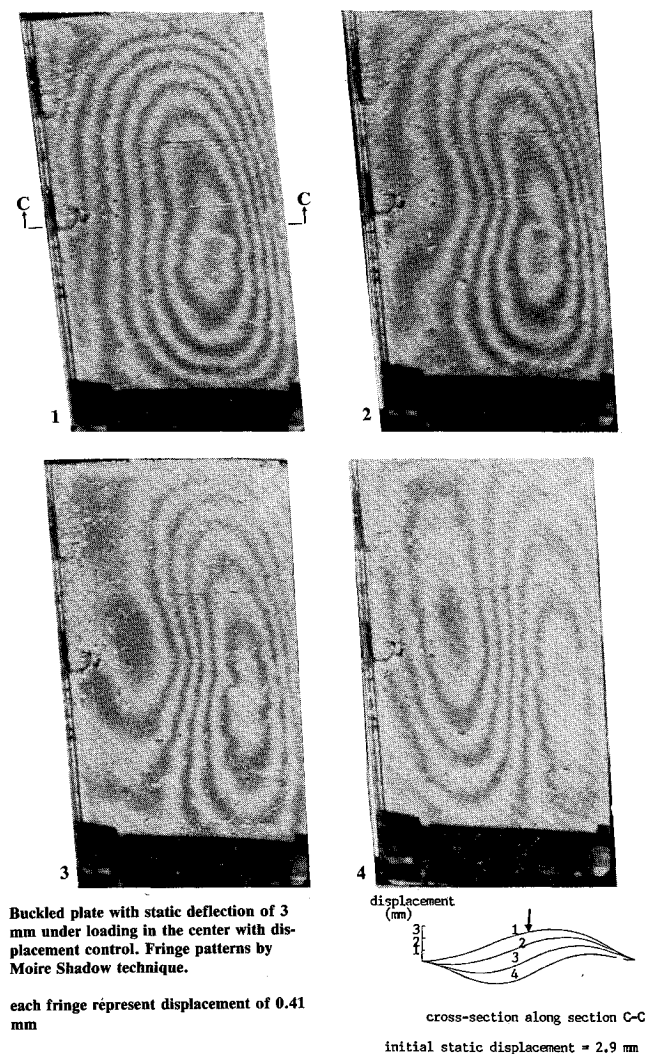


Fig. 14 The deformation patterns of snap-through of a buckled plate.

(Fig. 15) is similar to that of postbuckled plates. The low-frequency range (1.25–5 Hz; 0 Hz is not analyzed) dominates the spectrum when the snap-through motion is intermittent at an SPL of 152 dB, and the fundamental modal response at 130 Hz is much lower. However, the response in the frequency range of 5–50 Hz increases rapidly as SPL is increased. At an SPL of 160 dB, the spectrum has a minor peak of 43 Hz but does not vary a lot in the range of 0–50 Hz. This agrees with the prediction that snap-through motions are initiated for the frequency band lower than the fundamental frequency for high excitation level, as described earlier (Fig. 3). More theoretical and experimental work is planned to understand fully the snap-through motion in cylindrical panels.

Conclusions

From the theoretical and experimental results, the general characteristics of persistent snap-through motion in buckled plates are as follows:

- 1) The mean value of the response is much reduced from the initial static value and is equal to the mean of the two opposite static values.
- 2) The rms response is comparable to the initial static value when the snap-through motion is continuous.
- 3) The snap-through motion is most readily excited by excitation of frequency at a fraction of the fundamental frequency. The resulting response spectrum is dominated by frequencies less than the fundamental frequency.
- 4) The existence of snap-through causes large and sudden increases in the dynamic response of curved panels that can be much larger than those obtained in flat panels and can be more significant than other complicating effects, such as nonlinear damping and multimodal contribution.

The latter two characteristics are also found in cylindrical panels. These characteristics are all totally different from the stable dynamic motion of linear, hardening-spring, or softening-spring behavior as they all involve instability motion. The use of the single-mode analysis helps one to interpret and understand these characteristics easily. However, improvements with use of time integration techniques and inclusion of a few more modes are necessary.

The effect of snap-through motion is not considered in current sonic fatigue design practice. The concept that curved panels are stiffer than flat ones is not valid due to the possibility of snap-through. The design principle based on avoiding snap-through motion is not reasonable because it is difficult to avoid snap-through for low curvature. For further experimental and theoretical work, it is necessary to predict the upper limit of the no-snap-through region for very curved plates, and it is also important to predict the response magnitude with continuous snap-through in mildly curved plates.

Appendix

The transverse displacement of a plate under in-plane compression is

$$w = Q\phi(x, y) \quad (A1)$$

where Q is the modal displacement and $\phi(x, y)$ is the shape function for transverse displacement; e.g., $\phi(x, y) = (1 - \cos 2\pi x/a)(1 - \cos 2\pi y/b)$ for clamped plates, where a is length and b is width.

The equation for bending strain energy is

$$U_B = \frac{1}{2} K Q^2 \quad (A2)$$

where K is a constant depending on plate properties and $\phi(x, y)$.

The tensile strain, x direction, is

$$\begin{aligned} \epsilon_x &= \frac{-u}{a} + \frac{1}{2} \left(\frac{\partial w}{\partial x} \right)^2 \\ \epsilon_x &= \frac{-u}{a} + \frac{1}{2} \left(\frac{\partial \phi}{\partial x} \right)^2 Q^2 \end{aligned} \quad (A3)$$

From Eq. (A1) $-u/a$ is the strain due to edge shortening u . Similarly,

$$\epsilon_y = \frac{1}{2} \left(\frac{\partial \phi}{\partial y} \right)^2 Q^2 \quad (A4)$$

(assuming no edge displacement).

From Eqs. (A3) and (A4) and integrating the strain energy over the volume, the tensile strain energy is given by

$$U_T = \frac{1}{2} \left(T_1 u^2 - T_2 u Q^2 + \frac{1}{2} T_3 Q^4 \right) \quad (A5)$$

where T_1, T_2, T_3 are constants depending on plate properties and $\phi(x, y)$.

Using $\partial(U_B + U_T)/\partial Q = P$ (P being the modal force), from Eqs. (A2) and (A5),

$$KQ - T_2 u Q + T_3 Q^3 = P \quad (A6)$$

putting $u_c = K/T_2$ (u_c being the value of u at the buckling point)

$$Q_p^2 = B/T_3 (Q_p = Q \text{ at } u = 2u_c)$$

$$q = Q/Q_p, \quad p = P/KQ_p$$

Dividing Eq. (A6) by KQ_p and using the preceding substitution, the nondimensional equation is obtained:

$$q - (u/u_c)q + q^3 = p$$

Acknowledgments

This work was done by the author as part of the Research Associateship Program of the National Research Council, and as a guest investigator in the Structural Acoustics Branch of the NASA Langley Research Center. Advice from John Mixson and Sherman Clevenson and the assistance of Tracy Miller were very helpful to the research work.

References

- ¹Mei, C. and Wolfe, H. F., *On Large Deflection Analysis in Acoustic Fatigue Design. Random Vibration-Status and Recent Developments*, I. Elishakoff and R. H. Lyon (ed.), Elsevier, Amsterdam, 1986, pp. 279–302.
- ²Vaicaitis, R., Jan, C. M., and Shinozuka, M., "Nonlinear Panel Response from a Turbulent Boundary Layer," *AIAA Journal*, Vol. 10, April 1972, pp. 895–899.
- ³Mei, C. and Prasad, C. B., "Effect of Large Deflection and Transverse Shear on Response of Rectangular Symmetric Composite Laminates Subjected to Acoustic Excitation," *Proceedings of the AIAA/ASME/ASCE/AHS 28th Structures, Structural Dynamics, and Materials Conference*, AIAA, New York, 1987, pp. 809–826.
- ⁴White, R. G., "Comparison of the Statistical Properties of the Responses of Aluminum Alloy and CFRP Plates to an Acoustic Excitation," *Composites*, Oct. 1978, pp. 251–258.
- ⁵Wentz, K. R. and Mei, C., "Experimental Nonlinear Response of Plates Subjected to High Intensity Noise," *AIAA Paper 81-0631*, April 1981.
- ⁶Jacobson, M. J. and Maurer, O. F., "Oil Canning of Metallic Panels in Thermal-Acoustic Environment," *AIAA Paper 74-982*, Aug. 1974.
- ⁷Holehouse, I., "Sonic Fatigue Design Techniques for Advanced Composite Aircraft Structures," *Air Force Wright Aeronautical Lab-*

oratories, Wright-Patterson AFB Ohio, TR-80-3019, 1980.

⁸Ng, C. F. and White, R. G., "The Dynamic Behavior of Postbuckled Composite Plates Under Acoustic Excitation," *Composite Structures*, Vol. 9, Jan. 1988, pp. 19-35.

⁹Jacobson, M. J., "Sonic Fatigue of Advanced Composite Panels in Thermal Environments," *Journal of Aircraft*, Vol. 20, March 1983, pp. 282-288.

¹⁰Yamaki, N. and Chiba, M., "Nonlinear Vibrations of a Clamped Rectangular Plate with Initial Deflection and Initial Edge Displacement," *Thin-Walled Structures*, Vol. 1, Jan. 1983, pp. 3-29.

¹¹Tseng, W. Y. and Dugudji, J., "Nonlinear Vibrations of a Buckled Beam Under Harmonic Excitation," *Journal of Applied Mechanics*, June 1971, p. 647.

¹²Seide, P., "Snap-Through of Initially Buckled Beams Under Uniform Random Pressure," *Proceedings of 2nd International Conference in Recent Advances in Structural Dynamics*, Southampton, England, April 1984, pp. 300-312.

¹³Ng, C. F., "The Analysis of Non-Linear Dynamic Behavior (Including Snap-Through) of Postbuckled Plates by Simple Analytical Solution," NASA TM-89165.

¹⁴Jacobson, M. J., "Effect of Structural Heating on the Sonic Fatigue of Aerospace Vehicle Structures," Air Force Flight Dynamics Laboratory, TR-73-56, Jan. 1974.

¹⁵Ng, C. F., "Behavior of Postbuckled Composite Plates Under Acoustic Excitation," Ph.D. Thesis, University of Southampton, Southampton, UK, 1986.

*Recommended Reading from the AIAA
Progress in Astronautics and Aeronautics Series . . .*



Thermal Design of Aeroassisted Orbital Transfer Vehicles

H. F. Nelson, editor

Underscoring the importance of sound thermophysical knowledge in spacecraft design, this volume emphasizes effective use of numerical analysis and presents recent advances and current thinking about the design of aeroassisted orbital transfer vehicles (AOTVs). Its 22 chapters cover flow field analysis, trajectories (including impact of atmospheric uncertainties and viscous interaction effects), thermal protection, and surface effects such as temperature-dependent reaction rate expressions for oxygen recombination; surface-ship equations for low-Reynolds-number multicomponent air flow, rate chemistry in flight regimes, and noncatalytic surfaces for metallic heat shields.

TO ORDER: Write AIAA Order Department,
370 L'Enfant Promenade, S.W., Washington, DC 20024

Please include postage and handling fee of \$4.50 with all orders.
California and D.C. residents must add 6% sales tax. All orders under
\$50.00 must be prepaid. All foreign orders must be prepaid. Please allow
4-6 weeks for delivery. Prices are subject to change without notice.

1985 566 pp., illus. Hardback
ISBN 0-915928-94-9
AIAA Members \$49.95
Nonmembers \$74.95
Order Number V-96